On the charge overcompensation of quenched polyelectrolyte stars electrostatically adsorbed onto a quenched oppositely charged planar surface

F. A. M. Leermakers[a] and J. M. P. van den Oever
Laboratory of Physical Chemistry and Colloid Science, Wageningen University, Dreijenplein 6, 6703 HB Wageningen, The Netherlands

E. B. Zhulina
Institute of Macromolecular Compounds of the Russian Academy of Sciences, 199004 St. Petersburg, Russia and The University of Texas at Austin, Department of Chemistry and Biochemistry and Center for Polymer Research, Austin, Texas

(Received 3 June 2002; accepted 9 October 2002)

We present numerical self-consistent field calculations in a two-gradient cylindrical coordinate system for a (translationally restricted) quenched polyelectrolyte star which is electrostatically attracted to an oppositely charged surface with homogeneous surface charge density at a given ionic strength of a 1:1 electrolyte. The results prove that without any additional driving force for adsorption, electrostatic attraction alone can give significant overcompensation of the surface charge provided that the ionic strength is below some critical value. This is demonstrated for the case that the charge density on the surface is lower than the (projected) charge density in the star. In the regime of charge overcompensation, the thickness of the adsorbed layer is of the order of the star size in solution. The adsorbed layer is laterally inhomogeneous and the outer part of the adsorption profile is locally neutralized by the small counterions. © *2003 American Institute of Physics.*
[DOI: 10.1063/1.1526092]

I. INTRODUCTION

The classical mean-field theory for polyelectrolytes at interfaces correctly points out that the adsorption of polyelectrolytes onto oppositely charged interfaces is a spontaneous process. The driving force for this process is the entropy gain of the small ions in the system when they no longer are needed to screen the surface charge. The adsorbed amount is, as a consequence of this adsorption mechanism, a function of the concentration of 1:1 electrolyte in the solution. At high ionic strength, when the entropy gain of the small ions is less important, it is possible to displace the polymer from the interface.[1–6] At very low ionic strength the adsorption tends to saturate to a value for the adsorption that is very close to the exact surface charge compensation. Indeed, the exact surface charge compensation is expected at very low ionic strength. The classical mean-field theory for polyelectrolytes at interfaces thus cannot predict surface charge overcompensation. This failure is generally attributed to the fact that spatial correlations between charges are ignored. When, however, such correlations are taken into account, the overcharging is predicted for a variety of systems (see, for example, Ref. 7, and references therein). Also recent Monte Carlo simulations clearly show the charge overcompensation being a function of the linear charge density in relation to the surface charge density.[8]

Recent studies[9] demonstrated that spherical particles with number of charges $Z \gg 1$ (referred to as Z ions) form a two-dimensional highly correlated liquid when adsorbed on an oppositely charged background. By using the concept of the Wigner crystal to describe the short-range ordering of Z ions, the authors in Ref. 9 demonstrated that overcharging of the plane with surface charge density σ by a saturated adsorbed layer of Z ions is governed by the reduced charge on the particle $\zeta = Ze/\pi\sigma r_s^2$ where e is an elementary charge and r_s is the Debye screening length. When $\zeta \gg 1$, a noticeable overcompensation of surface charge is predicted. The nature of the Z ions is not essential for the overcompensation phenomenon. Hence, polyelectrolyte stars, spherical micelles, or other charged objects with spherical symmetry can be envisioned as Z ions as well. One therefore expects that similar to small Z ions, adsorbed polyelectrolyte stars and spherical micelles would form a correlated liquid-like pattern and overcharge the surface. Recent experimental findings[10] are in line with these expectations.

In contrast to small Z ions, polyelectrolyte stars and micelles have reduced conformational degrees of freedom near the surface. Therefore, the structure of the adsorbed layer is governed by both electrostatic and conformational contributions. Another important difference is the possible condensation of counterions into the interior of the star or the corona of micelle. This effect is counteracted by the repulsion of the counterions of the star from the charged surface. As a result, the effective charge on the star or micelle (Z) becomes dependent on, e.g., the number of branches, the degree of ionization and the distance from the surface.

In this study it is demonstrated that a numerical self-consistent field (SCF) model, where density gradients in two

[a]Electronic mail: frans.Leermakers@wur.nl

directions are accounted for, can successfully be implemented to investigate the overcharging phenomena in adsorption of polyelectrolyte stars. Due to the spherical symmetry of charged stars and their strongly correlated positioning on the surface, the two-gradient SCF model is sufficient to mimic the adsorbed stars near an oppositely charged interface. By using a two-gradient model we account for spatial lateral correlations between neighboring stars and determine the distributions of all the components in both lateral and normal directions.

The remainder of this paper is organized as follows: In Sec. II we start with the scaling analysis of the effective star charge Z and formulate the two-gradient SCF model in detail. Thermodynamic rules are presented that help us to identify the plateau of the adsorption isotherm of stars on oppositely charged surfaces. In Sec. III will elaborate on a particular example rather than giving a complete analysis of the problem. Both the behavior of stars at the interface as well as in the solution will be investigated. A short discussion and our conclusions are formulated at the end of the paper.

II. MODEL

A. Charge renormalization

We start with brief scaling analysis to determine the effective charge on a polyelectrolyte star positioned in the electric field of a charged surface. Consider a star-like polymer comprising f flexible branches of N_P monomers with linear dimension a. Let $\alpha \ll 1$ be the degree of ionization so that the net charge on the star is $Q=\alpha f N_P$. We model such a star by a sphere of radius R with averaged charge density $(=Q/R^3)$. If the star contains $(Q-n)$ counterions, the effective charge Z is given by $Z=en$. The center of the star is located at distance D from the oppositely charged surface with surface charge density σ. The charged surface with its counterions creates an electric field and an electrostatic potential profile $\psi(z)$. The dimensionless electrostatic potential $\Delta\Psi=e\Delta\psi/k_BT$ is given by[11]

$$\Delta\Psi(z)=-2\ln\left[\frac{1-\gamma\exp(-z/r_s)}{1+\gamma\exp(-z/r_s)}\right], \tag{1}$$

where

$$\gamma=\frac{\Lambda/r_s-\sqrt{(\Lambda/r_s)^2+1}+1}{\Lambda/r_s+\sqrt{(\Lambda/r_s)^2+1}-1}. \tag{2}$$

Here

$$\Lambda=\frac{1}{2\pi l_B\sigma} \tag{3}$$

is the Gouy–Chapman length and $l_B=e^2/\epsilon k_BT$ is the Bjerrum length. At distances $z \gg r_s$, $\Delta\Psi(z)\sim\exp(-z/r_s)$, and the effect of the charged surface is negligible. At distances $z \ll r_s$, the expansion of $\Delta\Psi(z)$ with respect to the small parameter $z/r_s \ll 1$ gives the following expressions for the electrostatic potential. When $\Lambda/r_s \ll 1$, then $\gamma\approx 1-\Lambda/r_s$ and

$$\Delta\Psi(z)\approx -2\ln\left(\frac{z+\Lambda}{2r_s}\right), \tag{4}$$

whereas when $\Lambda/r_s \gg 1$ and $\gamma\approx r_s/2\Lambda$,

$$\Delta\Psi(z)\approx\frac{2r_s}{\Lambda}. \tag{5}$$

The free energy of a star with its center located at distance $z=D>R$ yields

$$\Delta F/k_BT=-n\Delta\Psi(D)+\frac{n^2}{R}l_B+n\ln(\varphi_s^b)+(Q-n)\ln\left[\frac{3(Q-n)}{4\pi R^3}\right]+f\frac{R^2}{a^2N}. \tag{6}$$

The first term in Eq. (6) is the electrostatic energy of a star with its $(Q-n)$ counterions in the external electric field created by an oppositely charged surface. The second term is the electrostatic self-energy due to the effective charge $Z=en$ of the star. The third term determines the translational entropy of n counterions that escaped from interior of the star and transferred to the bulk solution with concentration of salt φ_s^b, whereas the fourth term accounts for the translational entropy of the remaining $(Q-n)$ counterions spread uniformly inside the star. Finally, the last term is the elastic free energy due to the stretching of f branches of the star.

By minimizing ΔF with respect to two independent variables, n and R, and by retaining only the major contributions we find the following:

For large stars with number of branches

$$f \gg f_* \approx \frac{1}{\sqrt{\alpha}}\frac{a}{l_B}\left[\Delta\Psi(D)+\ln\left(\frac{r_s}{r_{\text{in}}}\right)\right] \tag{7}$$

the effective charge $Z=en \ll Q$, and the star retains the majority of the counterions. Here, $r_s=1/(8\pi l_B\sqrt{\varphi_s^b})$ is the Debye screening length controlled by the concentration φ_s^b of added salt, whereas $r_{\text{in}}=1/(8\pi l_B\sqrt{3Q/4\pi R^3})$ is determined by the average concentration of mobile counterions inside the star. The radius of the star R and the number of escaped counterions n are given, respectively, by

$$R\approx a\sqrt{\alpha}N_P \tag{8}$$

and

$$n\approx\frac{R}{l_B}\left[\Delta\Psi(D)+\ln\left(\frac{r_s}{r_{\text{in}}}\right)\right]. \tag{9}$$

For small stars with $f \ll f_*$, nearly all counterions leave the star, and the branches are stretched due to the unscreened electrostatic repulsion. Here,

$$n\approx\alpha f N_P \tag{10}$$

and

$$R\approx\frac{n^{2/3}N_P{}^{1/3}}{f^{1/3}}(a^2l_B)^{1/3}\approx\alpha^{2/3}f^{1/3}N_P(a^2l_B)^{1/3}. \tag{11}$$

In the absence of a charged surface, $\Delta\Psi(D)=0$, the results coincide with earlier findings.[12]

It is seen from Eq. (9), that the effective charge Z is noticeably affected by the presence of a charged surface only when $\Delta\Psi(D)$ becomes comparable to the entropic gain due to the release of the counterions [the second term in square brackets in Eq. (9)]. Equations (4) and (5) indicate that $\Delta\Psi(D)>1$ only when $\Lambda/r_s \ll 1$. This case corresponds to low concentrations of added salt (high values of r_s) and/or highly charged surfaces (low values of the Gouy–Chapman length Λ). By substituting Eq. (4) in Eq. (9) we find that Z increases logarithmically as the star approaches the surface,

$$Z \approx e \frac{R}{l_B} \ln\left(\frac{2r_s}{D+\Lambda} \frac{r_s}{r_{\text{in}}} \right). \tag{12}$$

The effective charge Z increases logarithmically also with a decrease in salt concentration. In the limit $r_s \to \infty$, the star loses all its counterions. However, at finite salt concentrations, the dominant power law dependence $n \sim R/l_B$ ensures that the polyelectrolyte star retains the majority of counterions when the number of branches is high enough, i.e., $f \gg f_*$.

Up to now we considered a single star near an oppositely charged surface. The presence of surrounding stars additionally decreases the effective charge Z. To evaluate the effect qualitatively, we consider a star with k nearest neighbors each located at a lateral distance H from the central star. The free energy of the central star now comprises an additional term due to the electrostatic interaction with its neighbors,

$$\Delta W_{\text{int}}/k_B T = \frac{k n^2 l_B}{2H} g\left(\frac{H}{D} \right), \tag{13}$$

where the function $g(H/D)$ can be approximated by a power law dependence.[13] When $r_s > D > \Lambda$ and $X = H/D \ll 1$, the repulsion between stars is essentially unscreened, and $g(X) \simeq 1$. However, when $X = H/D \gg 1$, the interaction between stars is screened,[13] and then $g(X) \simeq X^{-2}$. At distances $D < \Lambda$, the screening length is given by Λ, and only stars found within a radius Λ from the central star contribute essentially to the interstar repulsion.

By adding $\Delta W_{\text{int}}/k_B T$ to the expression for the free energy, Eq. (6), and by minimizing ΔF with respect to n we find

$$n \approx \frac{R}{l_B \left[1 + \frac{kR}{2H} g\left(\frac{H}{D} \right) \right]} \left[\Delta\Psi(D) + \ln\left(\frac{r_s}{r_{\text{in}}} \right) \right]. \tag{14}$$

As is seen from Eq. (14), the effect of neighbors could be quite noticeable. For example, for $k=6$ (i.e., for triangular packing of neighboring stars) and $H=3R$, the effective charge Z can decrease by factor of 2. Moreover, at distances $D \ll R$ from the surface, we find [by substituting $D \simeq R$ in Eq. (14)] that the effective charge Z is almost constant as function of D and decreases with a decrease in distance between the stars, H.

In the following focus on relatively large stars (or starlike micelles) with a fixed number of chains $f > f_*$ and use the two-gradient SCF model to get insight into the adsorption of such objects.

B. Numerical SCF approach

As explained previously we consider, also in the numerical analysis, a surface with fixed charge density σ. The polymer stars with f arms, each of length N_P, have an opposite charge density of $\alpha = 1/m$ (m is the "distance" along the chain between unit charges). The volume fraction of 1:1 electrolyte (in the bulk) is given by φ_s^b. It is taken that it is possible to restrict the star with its center to a fixed position in space. This restriction-region is placed on the axis of a cylindrical coordinate system. The space in this cylindrical coordinate system is represented by a lattice with the following characteristics. Flat lattice layers are numbered in the direction along the axis of the cylinder $z = -1,0,1,2,\ldots,M_z,M_z+1$. In this lattice a surface with fixed properties is placed on the z = 0 coordinate. Between layers M_z and M_z+1 the mirror-like boundary conditions apply. This means that potentials as well as densities at M_z+1 are set equal to corresponding quantities at M_z. In the radial direction rings numbered $R = 1,2,\ldots,M_R,M_R+1$ are defined. The volume, i.e., the number of sites in each ring is given by $L(R) = \pi(R^2 - (R-1)^2) \propto R$. Between M_R and M_R+1 reflecting boundary conditions apply, similar to that explained for the mirror-like boundary condition in the z direction. Formally, this boundary condition is an approximation when the number of lattice sites is not a constant. The mirror-like boundary conditions simulate that the adsorbed stars are not isolated, in particular when M_R is finite (i.e., $M_R \approx R_g$ of the isolated star). In effect, the mirror-like boundary condition allows chain fragments to cross the boundary and enter the space of the neighboring stars. When this occurs a neighboring star will put a similar fragment into the central box. Such boundary condition, essential to mimic the effects of packing effects of stars near the surface, accounts reasonably well for the conformational entropy effects of overlapping and interacting stars. As told, the solid substrate occupies layer $z=0$ and the surface charge is homogeneously distributed. Nevertheless, it is also necessary to know how the electrostatic potential profile is for $z<0$. One way to solve this problem is to introduce image charges. We choose to implement mirror-like boundary conditions between $z=-1$ and $z=0$. This means that the solid phase is just two layers wide, i.e., $z=-1,0$, and that the electrostatic potential ψ is the same in the pairs of coordinates $\psi(-1,R) = \psi(0,R)$ for all R. With this ansatz it is exactly known how the electrostatic boundary conditions are and the overhead in calculation time and computer memory requirements is minimal. This method may represent, e.g., a very thin clay platelet.

The value of R_M determines the area per chain on the surface: $A_s = A(M_R) = \pi M_R^2$. There is just one polyelectrolyte chain per area A_s and thus the value of M_R also fixes the adsorbed amount. Alternatively, one can think of the existence of a characteristic distance, H, between stars along the surface to be twice the value of M_R.

The reflecting boundary conditions at M_z implies that there is a second surface placed a distance $2M_z$ from the first one. The value of the system size (M_z, M_R) is limited for computational reasons. It is necessary to realize that there

may always be some perturbations on the thermodynamic quantities from finite system-size effects. We will return to this problem in the following.

The polyelectrolyte star is restricted with the first segment of each arm to be at a fixed z_g coordinate. This first segment is also restricted in the radial coordinate $R \leqslant R^* \approx 1$. A finite R^* value is needed to host up to $f^{\max}=\pi(R^*)^2$ arms. We will denote the grafting distance by the parameter $D=z_g$.

The strategy on which the SCF theory is based is well-known. For each segment type there exists a segment potential conjugated to the segment densities. The segment densities obey an incompressibility constraint,

$$\sum_A \varphi_A(z,R)=1, \tag{15}$$

for each coordinate. In Eq. (15) the subindex A refers to all segment types in the system. There are of course monomeric components, i.e., $A=\mathrm{W}^{(0)},\mathrm{Na}^{(1)},\mathrm{Cl}^{(-1)}$, where the superindex indicates the valency ν of the units. Here W represents the solvent (water), and the other two quantities are the two ions. In addition, there are charged unit of the polymer, i.e., $P^{(1/m)}$, and if a surface is present the surface units are represented by $S^{(-\sigma)}$. We will assume that the system is ideal, i.e., that nonelectrostatic interactions are absent in the system and that the dielectric constant in the system is homogeneous, i.e., $\epsilon=80$. In this approximation the (normalized) selfconsistent potential for a given segment type A is given by

$$u_A(z,R)=u'(z,R)+\nu_A\Psi(z,R) \tag{16}$$

indicating two contributions. The first one is associated with the work that needs to be done to create on coordinate (z,R) space to insert a monomer A in the system. The second term is the classical electrostatic contribution (here in dimensionless units).

The distribution of the monomeric components is simply given by the Boltzmann weight

$$\varphi_{A'}(z,R)=\varphi^b_{A'}e^{-u_{A'}(z,R)}, \tag{17}$$

where A' is a monomeric quantity. The distribution of the neutral solvent may be used to specify the excluded-volume potential

$$u'(z,R)=\ln\frac{\varphi^b_W}{\varphi_W(z,R)}, \tag{18}$$

where $\varphi^b_W=1-2\varphi^b_s$.

A polymer chain with segment ranking numbers $s=1,\ldots,N_P$ is grafted with $s=1$ in the range $(z=D,0<R\leqslant R^*)$. The distribution of a particular segment of a particular arm is given by

$$\varphi_P(z,R;s)=\frac{1}{G_N}\frac{G(z,R;s|D,0<R\leqslant R^*;1)G(z,R;s|N_P)}{G_P(z,R)}. \tag{19}$$

Because there are f arms the distribution of star segments is $\varphi_p(z,R)=f\Sigma_s\,\varphi_p(z,R;s)$. The normalization $C_P=1/G_N$ is given by

$$G_N=\sum_z\sum_R L(R)G(z,R;1|N_P). \tag{20}$$

It may be referred to as the single arm partition function as it contains the combined statistical weight to find the arm of length N_P in the system. This quantity is related to the chemical potential of the star as we will discuss in the following. In Eq. (19), which is the classical composition law, two complementary end-point distribution functions are introduced. The first one is the distribution function which starts with segment number one in the restriction coordinates. The second one is the distribution function of chain fragments that start at the free end $s=N_P$. The corresponding propagators are

$$\begin{aligned} G(z,R;s|D,0<R\leqslant R^*;1) &= G_P(z,R)\langle G(z,R;s-1|D,0<R\leqslant R^*;1)\rangle,\\ G(z,R;s|N_P) &= G_P(z,R)\langle G(z,R;s+1|N_P)\rangle, \end{aligned} \tag{21}$$

with starting conditions $G(z,R;1|D,0<R\leqslant R^*;1)=G_P(z,R)\,\delta(z,D;R\leqslant R^*)$ and $G(z,R;N_P|N_P)=G_P(z,R)$, respectively, where the $\delta(z,D;R\leqslant R^*)=1$ when $z=D$ and $R\leqslant R^*$ and zero otherwise.

The angular brackets in Eq. (21) express the geometry-dependent averaging of the end-point distribution function

$$\langle X(z,R)\rangle=\sum_{\rho=-1,0,1}\sum_{\xi=-1,0,1}\lambda(z,\xi;R,\rho)X(z+\xi,R+\rho), \tag{22}$$

where $\lambda(z,\xi;R,\rho)$ is the *a priori* transition probability to go from a site (z,R) to $(z+\xi,R+\rho)$. In a cubic lattice each site has six neighbors. For very large values of R the limiting flat lattice results are $\lambda(z,\xi;R,\rho)=\lambda_1=1/6$ for $(\xi,\rho)=(-1,0),(1,0),(0,-1),(0,1)$, and $\lambda(z,0;R,0)=2/6$. The "diagonal" steps $(\xi,\rho)=(-1,-1),(1,1),(1,-1),(-1,1)$ obtain the probability zero. For small values of R, the curvature is important and consequently the transition probabilities depend on the R coordinate. Simple geometric arguments lead to $\lambda(z,0;R,1)=\lambda_1 2\pi R/L(R)$, $\lambda(z,0;R,-1)=\lambda_1 2\pi(R-1)/L(R)$ and $\lambda(z,0;R,0)=1-2\lambda_1-\lambda(z,0;R,-1)-\lambda(z,0;R,1)$.

It can be shown that

$$\langle X(z,R)\rangle-X(z,R)\approx\left(\frac{\partial^2}{\partial z^2}+\frac{1}{R}\frac{\partial}{\partial R}\right)X(z,R). \tag{23}$$

The surface in the system is located at $z=0$ and the surface component S has a fixed distribution in space, i.e., it has a volume fraction $\phi_S(0)=\delta(z,0)$. When the volume fraction profiles of all other units in the system is known, it is possible to evaluate the charge distribution

$$q(z,R)=eL(R)\sum_A \varphi_A(z,R)\nu_A, \tag{24}$$

where ν_A is the valency of segment type A, the values of these have been mentioned earlier. It is convenient to define

also a dimensionless overall charge density $\tilde{q}(z,R) = q(z,R)/(eL(R))$. The charge distribution should be consistent with the Poisson equation

$$\left(\frac{\partial^2}{\partial z^2} + \frac{1}{R}\frac{\partial}{\partial R}\right)\psi(z,R) = -4\pi\frac{q(z,R)}{\varepsilon}. \tag{25}$$

The discretization of this equation may be expressed with the use of Eq. (22):

$$6(\langle\psi(z,R)\rangle - \psi(z,R)) = -4\pi\frac{q(z,R)}{\varepsilon}, \tag{26}$$

where the constant charge at the surface determines that the field lines go perpendicular to the surface. In all other system boundaries reflecting boundary conditions apply and this implies that the electric field $E=0$. It can be shown that the overall system is electroneutral (i.e., the charge in the space $0<z\leqslant M_z$, $0<R\leqslant M_R$ exactly compensates the surface charge).

A fixed point of the equations above-specified is found numerically with a precision of at least seven significant digits. When such a solution is found, it is possible to evaluate the thermodynamic quantities.

C. Thermodynamic definitions

The chemical potentials or the monomers $\mu_{A'} \equiv (\mu_{A'} - \mu^{\#}_{A'})/k_BT$ are straightforwardly found from

$$\mu_{A'} = \ln \varphi^b_{A'}, \tag{27}$$

where $A' = \mathrm{Na}^+$, Cl^-, W and the superindex b indicates the bulk value.

The free energy (Helmholtz energy) of the system follows from the logarithm of the canonical partition function. When short-range nearest-neighbor interactions are absent, the free energy $F \equiv (F - F^{\#})/k_BT$ is found from

$$F = \sum_z \sum_R L(R)\left[\sum_A \frac{\varphi_A(z,R)}{N_A}\ln(C_A N_A) + \ln\frac{\varphi_W(z,R)}{\varphi^b_W} - \frac{q(z,R)\psi(z,R)}{2L(R)k_BT}\right]. \tag{28}$$

The free energy is not the appropriate thermodynamic potential for the system. To understand this it is necessary to remember that in the following calculations the bulk concentrations of the small molecules $A' = \mathrm{W}$, Na^+, Cl^- are fixed. This means that a partial open free energy F^{po} defined as

$$F^{\mathrm{po}} = F - \sum_{A'} \sum_z \sum_R L(R)\varphi_{A'}(z,R)\mu_{A'} \tag{29}$$

is more appropriate. In this equation the summations are needed simply to find the number of molecules of type $A' = \mathrm{Na}^+$, Cl^-, W in the system.

It is essential to realize that in the SCF calculations the star is always modeled with a fixed position of the branching point. This means that the star has no translational degrees of freedom. This has major consequences for the thermodynamic analysis of the system. The primary goal is to estimate the maximum adsorbed amount of the stars on the surface. This plateau of the adsorption isotherm may be defined as the number of chains per unit area for the case that the concentration of the stars in solution is so high that the translational entropy of the stars in solution can be ignored, i.e., the system is near the overlap concentration. In this limit, the chemical potential of the stars in the bulk may be identified by Eq. (29) applied to the analysis of a star in the absence of a solid surface (i.e., in the bulk). For more dilute solutions of stars, we should add an ideal gas-like term to the (dimensionless) chemical potential of the stars in the bulk:

$$\mu_{\mathrm{star}} = \ln \varphi_{\mathrm{star}} + F^{\mathrm{po}}, \tag{30}$$

where φ_{star} is the volume fraction occupied by stars in the solution. Again, near the overlap concentration $\varphi_{\mathrm{star}} \approx 1$.

Finally, it is necessary to present an equation to evaluate the grand potential of the system in which the charged surface is in contact with an aqueous solution of small 1:1 electrolyte only

$$\Omega = \sum_z \sum_R \left[L(R)\ln\frac{\varphi_W(z,R)}{\varphi^b_W} - \frac{q(z,R)\psi(z,R)}{2k_BT}\right]. \tag{31}$$

This grand potential may be identified by $\Omega = \gamma A_s$, where $A_s = \pi M_R^2$ is the area of the surface of the system of interest and γ the surface tension. In the absence of charges no density gradients develop and the reference value of the surface tension is found, i.e., $\gamma = 0$.

III. RESULTS

A. Parameters

In this study the following (default) problem is considered. A surface with fixed surface charge density is $\sigma = -0.02$, i.e., one of 50 sites is on average charged by an elementary charge e. The charge is thought to be homogeneously distributed, i.e. it cannot adjust in any way to the conditions of the solution near to the surface. The concentration of small positively charged ions in the bulk is set equal to the concentration of the small negatively charged ions in the bulk φ^b_s. The polyelectrolyte is a star with $f=20$ arms. For this value of the number of arms it suffices to fix $R^* = 3$. Each arm has a length of $N_P = 100$ segments. Every tenth segment in the arm is charged, i.e., $m=10$, however it is assumed that the charge is homogeneously distributed [each segment in the star has a fractional charge $\alpha = 0.1$ ($m = 10$) of elementary charge].

The size of a lattice site was set to $\ell = 0.5$ nm, dielectric permittivity is homogeneous throughout the system $\epsilon = 80$, and the temperature is set to $T = 300$ K.

The ionic strength φ_s is a variable in the system. Very low values of φ_s will require large system sizes. Without mentioning otherwise a value of $\varphi_s = 10^{-4}$ is used. The second variable is the distance D the center of the star is placed away from the surface (in units of lattice sites). Then, there are the two parameters that determine the system size, M_z and M_R. With M_z, the distance between the two surfaces is varied. Without mentioning otherwise we will use $M_z = 99$. With this size it is possible to vary the grafting distance D between values of $0 < D \leqslant 65$. Increasing D to larger values will imply progressively increasing interactions between

stars sitting on either side of the reflecting boundary at M_z. To remain on the safe side we report only data up to $D=50$.

The value of M_R has a default value of $M_R=50$. In this case the surface charge in the patch with area A_s is, in absolute value, smaller than the overall charge on the star. Variations of M_R implies changes in the adsorbed amount as explained earlier, the variation of the average lateral distance between stars, and the amount of surface charge (over) compensation. The smaller the value of M_R the larger is the overcompensation.

B. Reference states

The first problem that needs to be discussed is the polyelectrolyte star in the bulk. In this case the system size is chosen (almost) identical to the previously discussed default case ($M_z=99$, $M_R=50$). However, the boundary condition between layers $z=0$ and 1 is changed from adsorbing to reflecting, similar to the boundary condition near M_z and the chain is grafted in the middle of the system, i.e., at $z_g=50$. The bulk concentration of salt was set to $\varphi_s=10^{-4}$. It is necessary to report at this stage the chemical potential of the star. In this case $F^{\rm po}=-1310.52$, and thus the translationally restricted chemical potential assumes this value. Again, the translationally restricted chemical potential is the key quantity to determine the plateau of the adsorption in the system. Structural properties of the star will be discussed in the following. First we will consider the same star, but now in the presence of the surface.

The second reference problem is the charged interface in the presence of a 1:1 electrolyte. The value found for the surface tension for the default system (i.e., $\sigma=-0.02$, $\varphi_s=10^{-4}$) is $\gamma=0.0454$ in units k_BT per site.

C. The polyelectrolyte star near the surface

In the computations, the translational degrees of freedom of the star is restricted. Therefore it becomes necessary to know the relevant thermodynamic quantities as a function of the distance D of the central grafting point to the surface. The concentrations of the small ions were fixed again to the default value $\varphi_s=10^{-4}$.

In Fig. 1 results are presented for $F^{\rm po}$ as a function of D for a relatively large value of the distance between the stars $M_R=50$. The system size in the normal direction was $M_z=99$. For the ionic strength conditions of $\varphi_s^b=10^{-4}$ it is possible to obtain reliable results that are not affected by confinement effects for D values as large as $D=50$.

The value of $F^{\rm po}$ for very large ''grafting'' distance D is plotted in Fig. 1 by a horizontal dashed line. The value is found from the $F^{\rm po}$ value of the translationally restricted star in the bulk plus the grand potential Ω as found by Eq. (31). The curve shown in Fig. 1 approaches this limiting value as expected, because the translational entropy is ignored for each value of D.

D. The plateau of the adsorption

It is interesting to notice that $F^{\rm po}(D)$ has a minimum. This minimum is also rather deep (in units of k_BT). The minimum shows that the star is electrostatically attracted to the surface. The repulsion found for very small values of D is not unexpected because the many-armed star will experience conformational problems when the center of the star is very close to the surface. To obtain the structure of an adsorbed layer with a fixed adsorbed amount (i.e., defined by the value of M_R) with $\tilde{k}$ stars near the surface with area A, we should do the Boltzmann average over all possible positions of D. In this average, the chains that are positioned at a value of D that corresponds to the minimum, i.e., $D=D_{\rm min}$, will dominate. The procedure becomes more simple if the fluctuations around this $D_{\rm min}$ position are ignored. In the following we will only consider the case that all chains have exactly the same position to the surface. In this case $F^{\rm po}(D_{\rm min})$ is the dominant value needed to estimate the plateau of the adsorption. It is necessary to realize that $F^{\rm po}$ in the interfacial system has a contribution of the grand potential and the chemical potential of the star,

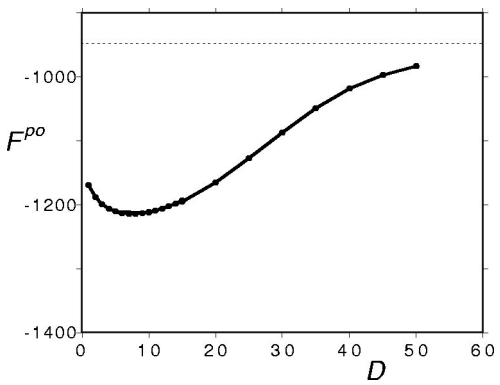

FIG. 1. The dimensionless free energy (partial open) $F^{\rm po}$ as a function of the distance D of the center of the star to the surface. The dashed line is the limiting value for $F^{\rm po}$ for large D values. $M_R=50$ and $M_z=99$.

$$F^{\rm po}(D)=\mu_{\rm star}(D)+\gamma(D)A_s. \tag{32}$$

It is convenient to normalize the free energy partial open to the value for very large D values,

$$\Delta F^{\rm po}(D)=\mu_{\rm star}(D)+\gamma(D)A_s-\mu_{\rm star}(\infty)-\gamma A_s, \tag{33}$$

where $\mu_{\rm star}(\infty)$ equals the translationally restricted value of the chemical potential in the bulk $\mu_{\rm star}$ and γ is the surface tension of the charged surface in the presence of 1:1 electrolyte only.

To estimate the plateau of the adsorption we should have the equality of chemical potentials of the stars in the bulk (translationally restricted) and stars positioned at $D_{\rm min}$. To obtain the latter, it is necessary to evaluate $\gamma(D_{\rm min})$ first. This value is found from numerical differentiation of $F^{\rm po}_{\rm min}=F^{\rm po}(D_{\rm min})$ with respect to the area A_s. This result is known when $F^{\rm po}_{\rm min}(M_R)$ is evaluated. Using this, it is relatively easy to see that when

$$\frac{\partial \Delta F^{\rm po}_{\rm min}/A_s}{\partial 1/A_s}=0, \tag{34}$$

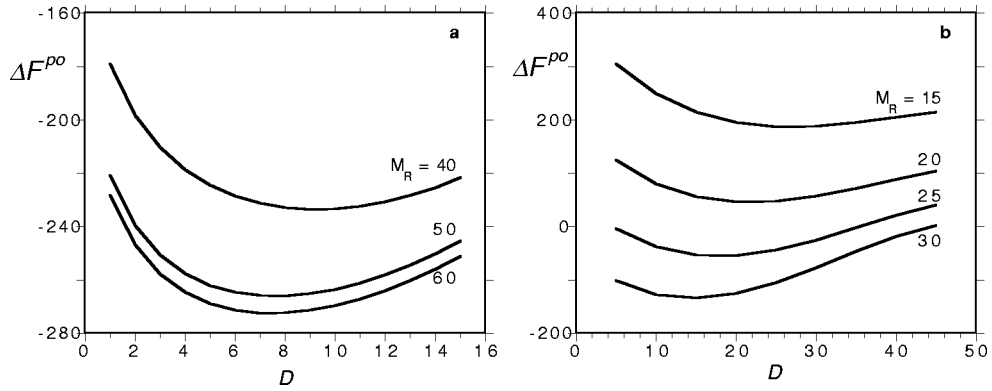

FIG. 2. Dimensionless and normalized free energy (partial open) ΔF^{po} as a function of the distance D of the star from the surface. The distance between the stars on the surface is controlled by the size of the system in the radial direction. (a) $M_R=40,50,60$, (b) $M_R=15,20,25,30$. The normalization of F^{po} is with respect to the value of F^{po} for very large values of D.

the chemical potentials of the chains in the adsorbed layer coincide with the translationally restricted chemical potential of the stars in solution. Thus Eq. (34) must be used to estimate the plateau of the adsorption isotherm.

In Fig. 2 results are presented for the free energy (partial open) as a function of the distance D of the grafting point of the star for a number of values of M_R. The value of the F^{po} plotted in Fig. 2 is normalized with respect the value of F^{po} for very large D.

In Fig. 2(a) the relevant part of the $\Delta F^{\mathrm{po}}(D)$ curve is given for values of $M_R=60$, 50, and 40. For these values, the stars are not yet strongly overlapping. As a consequence there exists a deep minimum of $\Delta F^{\mathrm{po}}(D)$ which shifts to larger values of D with decreasing distance between the stars. This is expected because smaller values of M_R mean higher values of adsorbed amount. A high adsorbed amount means thick adsorbed layers and thus the center of the star should be displaced away from the surface. Further, the minimum of $\Delta F^{\mathrm{po}}(D)$ becomes less deep with decreasing M_R.

In Fig. 2(b) the same system is considered for stars which are more densely packed on the surface. Indeed when $M_R=30$ or lower, we see the dramatic effect that the minimum of $\Delta F^{\mathrm{po}}(D)$ very quickly rises and does not remain negative for values of M_R smaller than approximately 25. This means that the system effectively reaches the plateau of the adsorption isotherm. Such high adsorbed amounts cannot be in equilibrium with isolated stars in solution. The interactions of stars in solution (the reference) has not been taken into account, and therefore it is found that $\Delta F^{\mathrm{po}}(D)$ does not approach the value zero for large values of D. Once more, to understand why $\Delta F^{\mathrm{po}}(D)$ does not go to zero for large D, one should realize that in the curves presented in Fig. 2 the value of M_R is fixed. Thus also when the star is far from the surface the curve of $\Delta F^{\mathrm{po}}(D)$ goes to the value which indicates the free energy change of the star when it is confined effectively into a cylinder with radius M_R. However, the star is not confined in the z direction. Therefore, the cases corresponding to $M_R \leqslant 25$ have no physical meaning.

Note that exact charge compensation occurs for $M_R=56.42$. This means that $M_R=60$ corresponds to a charge undercompensated system and all other systems presented in Fig. 2 are overcompensating the surface.

At this stage it is possible to estimate from the minima in the $\Delta F^{\mathrm{po}}(D)$ curves the plateau of the adsorption. In Fig. 3(a) the minimum of $\Delta F^{\mathrm{po}}(D)$ is plotted as a function of the distance between the stars M_R for the relevant range $30 \leqslant M_R \leqslant 40$. As anticipated from Fig. 2 this is a decreasing function. The same data are replotted in Fig. 2(b) but now in the coordinates $\Delta F^{\mathrm{po}}_{\mathrm{min}}/A_s$ versus $1/A_s$, where A_s is the area per molecule ($A_s=\pi M_R^2$). From this curve it is easily seen that the minimum occurs at $M_R=34$. In this point the

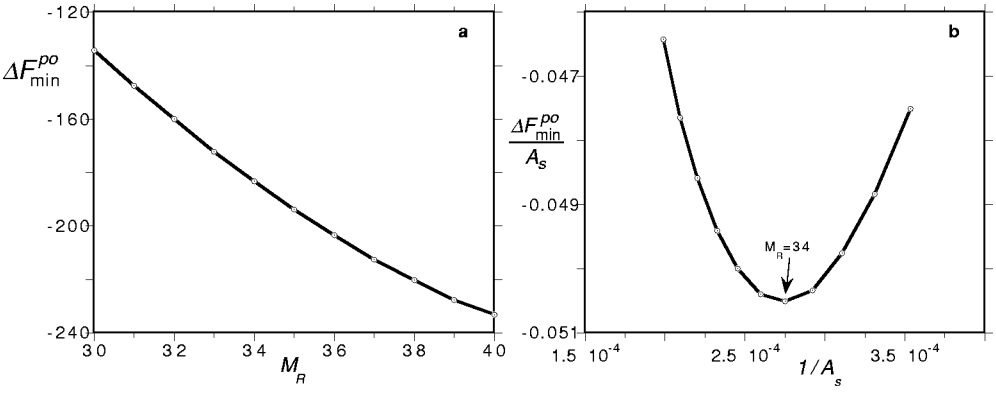

FIG. 3. (a) The minimum value of the $\Delta F^{\mathrm{po}}(D)$, $\Delta F^{\mathrm{po}}_{\mathrm{min}}$ as a function of the lateral distance between the stars M_R. (b) The $\Delta F^{\mathrm{po}}_{\mathrm{min}}$ divided by the area per molecule A_s vs the number of chains per unit area $1/A_s$. Parameters as in Fig. 2.

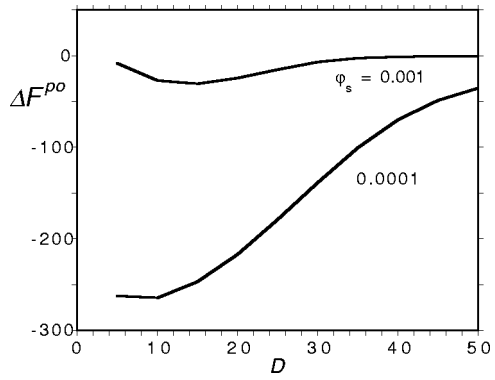

FIG. 4. The normalized dimensionless free energy partial open ΔF^{po} as a function of the distance D of two values of the ionic strength as indicated.

chemical potential of the adsorbed star equals exactly the translationally restricted chemical potential of a star in the bulk. This means that this point corresponds to the plateau of the adsorption isotherm. The total charge on the surface for $M_R=34$ is equal to -72.6 and thus the stars bring in a factor of 3 more charges to the surface than originally present on the surface. This amounts to a significant overcompensation of the charge.

Let us recall that the classical self-consistent field theory for polyelectrolyte adsorption typically predicts that electrostatically adsorbed polyelectrolytes have very flat adsorbed conformations. It is interesting to note that even for the case that the isotherm is not yet expected to be near the plateau of the adsorbed amount, the stars are not at all laying flat on the surface. This already follows from the fact that $D_{\min}>1$. Several arms of the star are not directed directly to the surface, but extend into the solution. One of the reasons for this novel behavior is that the charge density at the surface is significantly lower than the charge density in the polyelectrolyte star. There is no point for the star to reach out and stretch its arms very far away from its center in order to be closer to more charges on the surface. Neighboring stars, and also the 1:1 electrolyte, can more easily reach these charges and screen them.

Of course it is possible to force the star to lay more flat onto the surface. For example, when a ten times higher charge density on the surface is present, i.e., when the charge density on the surface is much larger than the projected charge density of the star, the minimum in the ΔF^{po} is very close to the surface. The density profiles (not presented) show that all the arms of the star are laying flat onto the surface, i.e., the adsorbed layer thickness is very thin (on the order of the segment size). The absolute value of ΔF^{po} is much larger than in the default system discussed in Fig. 2. This indicates that the adsorption is, as expected, much stronger in the case of high surface charge density.

Earlier in this paper it was anticipated that when adsorption is driven by electrostatic interactions, it should be possible to counteract this adsorption by the addition of salt. This effect is expected to occur as well for inhomogeneous adsorbed polyelectrolyte layers. To show that this is indeed the case, we present in Fig. 4 a result of F^{po} as a function of the distance D for the weakly laterally interacting case $M_R=50$ for two values of the ionic strength.

The result of $\varphi_s=10^{-4}$, which has already been presented in Fig. 1, is replotted in Fig. 4 in combination with the result for a tenfold higher ionic strength $\varphi_s=10^{-3}$. It must be mentioned that the normalization of the free energy partial open for the $\varphi_s=10^{-3}$ case is different from that of $\varphi_s=10^{-4}$. The reason for this is obvious. Both the surface tension of the charged interface in contact with the $\varphi_s=10^{-3}$ salt solution is now used as well as the free energy partial open of the bulk star in solution with a background ionic strength of $\varphi_s=10^{-3}$ has been applied.

Inspection of Fig. 4 indicates that the minimum in the ΔF^{po} shifted to much higher values and to larger D values. Both trends indicate that the stars have less surface affinity in the higher ionic strength conditions. In other words, the adsorption is highly suppressed. At even higher ionic strength, the minimum is found for positive values of ΔF^{po} (not shown). This means that there exists an ionic strength above which the star does not adsorb, i.e., there is a critical ionic strength for adsorption. This critical condition must also depend on the concentration of stars in solution. As a consequence, there also must exist a critical ionic strength above which the surface charge cannot be overcompensated. This is a significant observation as well.

E. Profiles and charge density characteristics

It is possible to present the charge distributions in the system. This will be done in the second part of this section. First it is of interest to discuss the effective charge Z of the star. In order to calculate this quantity, it is necessary to define the size of the star more accurately. A relative simplistic and effective way is to define the interior of the star to be the region where the polymer density is higher than some preset value: $\varphi_p>\varphi_p^{**}$. Then for the surroundings of the star it must be true that the polymer density $\varphi_p\leqslant\varphi_p^{**}$. After this, it is rather trivial to count the overall charges that are in the star interior, i.e., to estimate Z. In such an ansatz it will be clear that the interior volume of the star and also Z must depend on the value of φ_p^{**}. For this reason three values were chosen as indicated in Fig. 5(a). When $\varphi_p^{**}=10^{-2}$, approximately 1700 of the 2000 polymer segments of the star are counted to be within the star. When $\varphi_p^{**}=10^{-3}$ this value increases to about 1975 segments and for $\varphi_p^{**}=10^{-4}$ to 1998 segments are seen as interior segments. As can be seen in Fig. 5(a), these three ways to define the star size give qualitatively similar values for the effective charge. Even more important, each choice for φ_p^{**} gives a very similar behavior with respect to the variation of Z with the distance D.

In Fig. 5(a) it is shown that the effective charge Z increases significantly with decreasing D. For very large values of D, the effective charge goes to a constant value. This is already seen for the $\varphi_s=10^{-3}$ case, and the limiting values for the effective charge for the lower ionic strength of $\varphi_s=10^{-4}$ are indicated by the symbols plotted at $D=50$.

The fact that a nearly linear dependence for $Z(D)$ is found is not necessarily in contradiction with Eq. (12). In Eq.

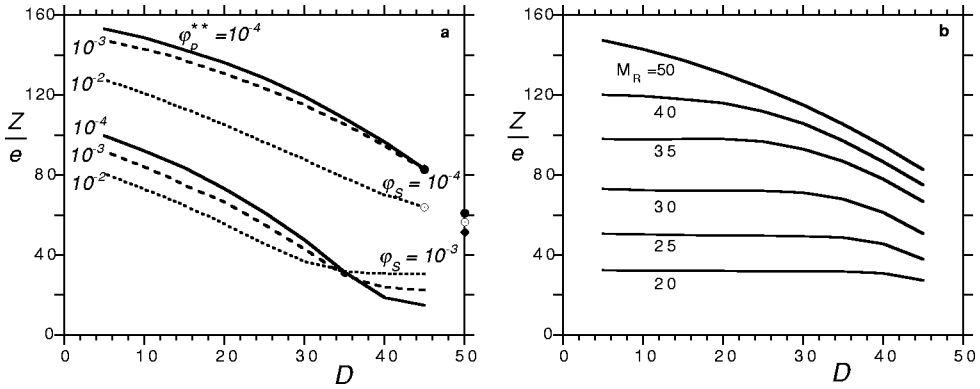

FIG. 5. (a) The effective charge in the star, $Z=ne$, as a function of the distance of the center of the star to the surface D for two values of the ionic strength $\varphi_s=10^{-4}$ and $\varphi_s=10^{-3}$ as indicated. For each ionic strength three results are plotted where a threshold value for the polymer density φ_p^{**} is used as indicated. In all curves $M_R=50$. (b) The effective charge in the star, Z, as a function of the distance of the center of the star to the surface D for six values of M_R as indicated. The threshold value for the definition of the star volume is fixed to $\varphi_s=10^{-3}$.

(12) a logarithmic dependence of Z with D is predicted in the range where $D>R$ and for small enough D values that the star is not much removed from the surface than the Debye length. For the conditions given in Eq. (5), the size of the star $R\approx 18$ (lattice units). At $D>45$, the electrostatic effects of the surface are not felt any more and thus only the region $20<D<45$ is operational to test the dependence of Eq. (12). This is a rather small range and no definite conclusions can be drawn from replotting Fig. 5(a) in the logarithmic coordinates (including using Λ).

The effective charge in the star as a function of the distance D for various values of the lateral distance between the stars M_R is given in Fig. 5(b). The value of $M_R=35$ is rather close to the plateau of the adsorption isotherm. With decreasing M_R, the amount of surface charge that is needed to be compensated by the star goes down. Therefore the effective charge in the star is a decreasing function of M_R. For values of $D<R$, the value of Z is independent of D for small values of M_R. This is completely in line with the scaling arguments mentioned previously [cf. Eq. (14)].

The effective charge increases when the distance of the star to the surface D decreases, especially for $D>R$. This trend was also anticipated. It is also clear that the correct trend is predicted for the effective charge as a function of the ionic strength. Decreasing the ionic strength increases the effective charge on the star.

In Fig. 6 a detailed comparison between the star in solution and at the surface is presented. In both cases the dimensions of the system were $M_R=50$ and $M_z=99$. The adsorbed star is placed with its grafting center at $D=10$, which is close to the optimal value. In Figs. 6(a) and 6(b) the contour plot of the polymer density is given. The charge density along the polymer is fixed, $m=10$, and thus the density of the charges due to the star is given by $\tilde{q}_P=\varphi_P/10$. In Figs. 6(c) and 6(d) the difference in positive and negative charges due to the 1:1 electrolyte is plotted. The difference between the charges due to the polymer and that due to the ions gives the (dimensionless) overall charge distribution, $\tilde{q}$, plotted in Figs. 6(e) and 6(f).

The density distribution of the star in the bulk [Fig. 6(a)] is essentially well known. In the central region the density

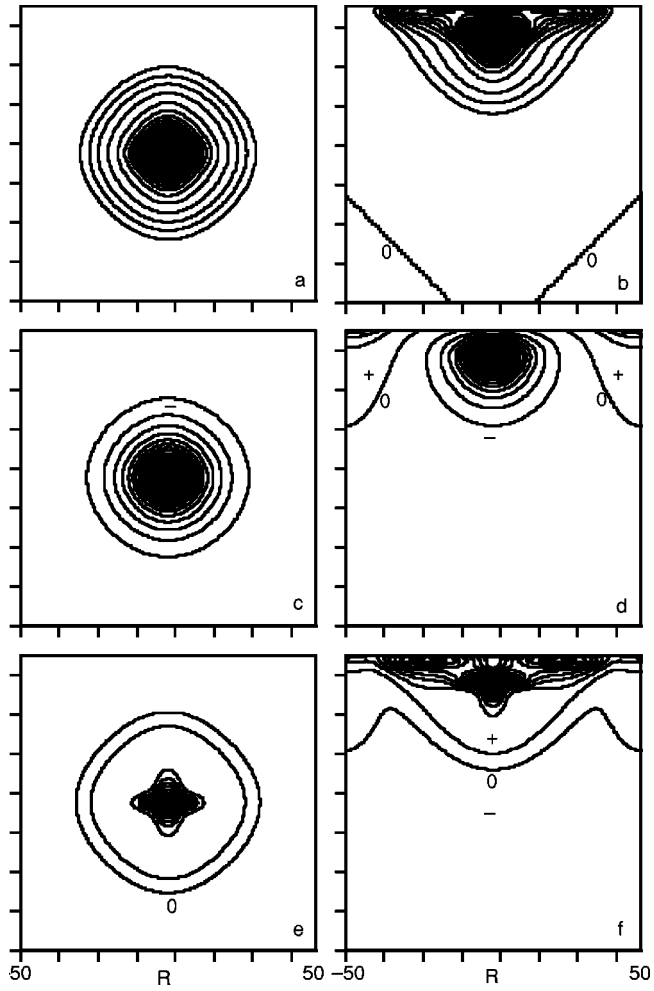

FIG. 6. (a), (c), (e) Characteristics of the star in the bulk with $M_R=50$ and $M_z=99$. (b), (d), (f) Characteristics of the star on the surface with $M_R=50$, $D=10$ and $M_z=99$. (a), (b) The overall distribution of polymer segments. The increments for the density for successive contour lines is $\Delta\varphi_P=0.005$. In (a) the outer contour line represents a polymer density of $\varphi_P=0.005$, in (b) the zero-density lines are also included. (c), (d) The difference in density of the positive ions and that of the negative ions $\varphi_{\mathrm{Na}}(z,R)-\varphi_{\mathrm{Cl}}(z,R)$. In (c) the outer contour line is $\varphi_{\mathrm{Na}}-\varphi_{\mathrm{Cl}}=-5\times10^{-4}$, and throughout the star the density of Na^+ is smaller than that of Cl^-. (e), (f) The total charge density distribution $q(z,R)$ (i.e., both for the star and the ions). The contour line with $q=0$ is indicated. The successive lines in (c), (f) have charge increments of $\Delta q=5\times10^{-4}$ and plus and minus signs indicate the positive and negative regions.

gradients are large and therefore there are many contour lines showing up as a black spot. In the periphery of the star the density drops almost linearly (equally spaced contour lines). The $\varphi_P = 0$ line is not reached in the box. This indicates that the star is weakly interacting with its neighbors. The contour lines are not perfectly spherical. This is due to some residual anisotropy in the lattice. Somewhat better results are possible when so-called optimized stencils are used.[14]

The density distribution of the star at the surface [Fig. 6(b)] is significantly different from that in the bulk. The star puts most of its arms near the surface and thus the arm-density on the outer part of the adsorbed layer is relatively low. This is the reason why the contour lines on the outer edge of the adsorbed star are spaced a bit further apart than in the bulk [cf. Fig. 6(a)]. The star at the surface also weakly interacts with its neighbors as may be judged from the density in between stars that drops to fairly low values. In between the stars, the polymer density is insufficient to locally compensate the surface charge.

The distribution of ions, in and around the stars are shown in Figs. 6(c) and 6(d) for the star in the bulk and on the surface, respectively. The distribution of these ions in the star has been discussed in the bulk system before and is well documented.[12] Except for the center of the star and the outermost region of the star, it is found that the ion distribution closely follows the polymer distribution. This phenomenon is known as the local charge neutralization which has been observed for (bulk) stars in the osmotic regime.[12] Significant differences between the distribution of ions and distributions of the polymer are found in the adsorbed state. Especially very close to the surface, the charge of the polymer chains is compensated by surface charges and not by the ions. Only at the periphery of the adsorbed star a local neutralization by small ions is observed, similarly as in the bulk. The counterions (the Cl^- ions) partition preferentially in the star, both in the bulk and near the surface. The surface is charged negatively and there are small regions in between the stars where the Na^+ ions dominate over the Cl^- ions. This is expected because in between the stars the Na^+ should screen the surface charge.

The overall charge distribution $\tilde{q}$ (the charge of the surface is not included) follows as discussed previously from the difference between the polymer charge and the charge coming from the 1:1 electrolyte. For the star in the bulk it is known that this difference is, except for the very center and the very edge of the star, almost constant. This explains why in Fig. 6(e) the contour plot for the overall charge distribution has a region where the equichargedensity lines are far apart. The overall charge has positive and negative regions. Inside the star it is positive and outside the stars it is negative. The $\tilde{q} = 0$ contour line is indicated. The ion distribution near a star on the surface, Fig. 6(f), also has a large region where the charge gradients are small. Interestingly the $\tilde{q} = 0$ contour line has a wave-like character lateral along the surface; the line is far from the surface for $R = R^*$ and, more surprisingly, at coordinates $R = \pm R_M$ and significantly closer to the interface in between these coordinates. The local dip in the $\tilde{q} = 0$ contour at approximately 3/4 the box size is due to the fact that just outside the adsorbed star the effective surface charge is negative whereas near the star this is positive. The dip reflects the spatial characteristics of the charge reversal. The charge distribution in the region $z > D$ is very similar to the distribution of the charge in the outer parts of the star in the bulk.

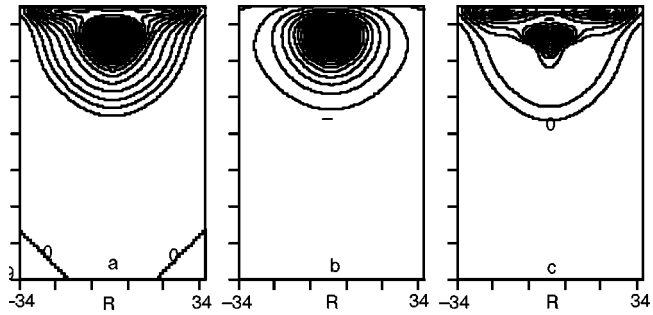

FIG. 7. (a) The overall distribution of polymer segments for a star near the surface as in Figs. 6(a) and 6(b). (b) The difference in density of the positive ions and that of the negative ions $\varphi_{Na}(z,R) - \varphi_{Cl}(z,R)$ as in Figs. 6(c) and 6(d). (c) The total charge density distribution in the solution as in Figs. 6(e) and 6(f). The "box" is defined by $M_R = 34$, $M_z = 99$, and $D = D_{min} = 12$. The value difference between the contour lines is the same as in Fig. 6.

For comparison it is of interest to present also the density and charge distribution for the interface saturated by stars. In Fig. 7 this system is presented where $M_R = 34$ and $D = 12$. It is seen that the thickness of the adsorbed layer is comparable to the size of the star in solution and that the star is strongly interacting with its neighbors. Nevertheless, the lateral density fluctuations remain significant, i.e., the periphery of the adsorbed layer is thicker on positions near the star center and is less thick in between the centers of the stars. Again the outer edge of the adsorbed layer resembles the structure and the charge distribution of free stars. Detailed comparison of the outer edge of the adsorbed layer with the radial density distribution of the isolated star in solution reveals small differences in the profile. These differences must be attributed to the lateral interactions between the stars and the fact that the star has an asymmetric distribution of its arms, i.e., there are more arms on the surface than pointing toward the solution. It is significant to mention that there are differences between the fully covered surface as shown in Figs. 7(a)–7(c) and the "starved" interface depicted in Figs. 6(b) and 6(d)–6(f). In the fully covered case the star compensates the surface charge everywhere along the surface. It was shown that this was not yet the case in the "starved" situation. The wave of the $\tilde{q} = 0$ line is more regular in the fully covered case. There is just one maximum distance (near the star center) and a local minimum half-way in between stars. Inspection of the Figs. 6(b) and 7(a) also shows that the thickness of the adsorbed layer increases with increasing coverage; the $\varphi_p = 0$ line shifted to larger z value in the fully covered case compared to the starved layer.

From the density profiles of the polymer stars it is rather trivial to evaluate the number of polymer segments that is in direct contact with the surface. This quantity is in principle experimentally accessible. Let us refer to it by the letter p. The contact number is obviously a function of the area available per start, M_R. Moreover it is a function of the distance

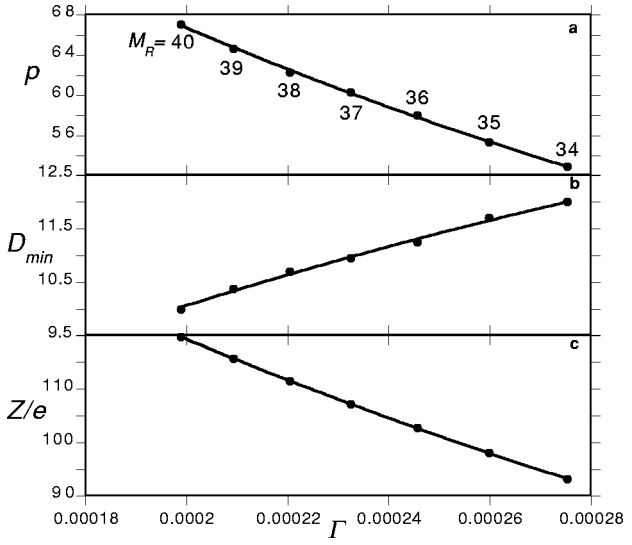

FIG. 8. The number of segments of the star being in direct contact with the surface p (a) and the effective charge Z (c) when the center of the star is at the optimal the distance $D_{\min}$ (b) to the surface as a function of the number of chains per unit area Γ. The lateral distance between the stars M_R is indicated in panel a for each point. The threshold value for the definition of the star volume (needed to compute Z) is fixed to $\varphi_p^{**}=10^{-3}$.

of the center of the star from the surface D. For each value of M_R there exists an optimal distance D where the free energy partial open F^{po} has a minimum. This value is plotted in Fig. 8(b). The number of surface contact for this optimal distance is presented in Fig. 8(a). To a good approximation it was found that D is a linear decreasing function of M_R in the interval investigated ($34 \leqslant M_R \leqslant 40$ corresponds to the adsorption corresponding to weakly starved layers up to full coverage). When the star is given more space on the surface, it is possible for the center to come somewhat closer to the surface. Correspondingly, the contact number p increases slightly more than linear with M_R [forcing a power-law dependence $p=(M_R)^{\alpha}$, a value of $\alpha=1.44$ was found]. The surface charge that is available for the star to ''compensate'' increases quadratically with M_R. Apparently the contact fraction cannot exactly follow this available surface charge. Note that the maximum value of the contact fraction is $p=2000$. This means that in all the cases shown in Fig. 8 the majority of the segments is not touching the surfaces. In Fig. 8(c) the effective charge Z is also presented as a function of the number of chains per unit area. With increasing adsorbed amount the effective charge goes down, in line with the results discussed earlier.

IV. DISCUSSION

We have shown that SCF theory can be successfully used to study the adsorption of polyelectrolyte stars and starlike micelles on oppositely charged substrates. We found that equilibrium adsorbed amount corresponds to noticeable overcompensation of the surface charge. We focused on the low ionic strength conditions when the Debye screening length was comparable to the size of an individual star (micelle). Under these conditions the classical one-gradient SCF theory predicts a slight undercompensation of the surface charge by adsorbed polyelectrolyte.[5] We found that in the framework of a two-gradient SCF model the equilibrium adsorbed amount near the plateau of the adsorption isotherm corresponds to noticeable overcompensation of the surface charge. To compare our results with predictions from Ref. 9 we estimate the effective charge Z for equilibrium surface coverage ($M_R=34$) as $Z \simeq 80$, whereas the overcharging given by $\sigma^*/\sigma=(Z/\pi M_R^2-\sigma)/\sigma$ as approximately 0.3. Our results indicate that for the set of parameters used in the SCF calculation, the overcompensation is lower than predicted in Ref. 9 approximately by a factor of 3. We attribute this difference to conformational restrictions imposed by the surface and neighboring stars.

In this paper we have shown that overcharging is possible when polyelectrolyte stars adsorb onto a charged interface. We expect that linear chains (two-armed stars) will also show this phenomenon. In recent years there has been extensive activity in the field of the formation of polyelectrolyte multilayers on (charged) surfaces.[15–18] These multilayers are formed by alternatingly presenting negatively- and positively-charged polyelectrolytes to a substrate. This can be done, e.g., by dipping a substrate into solutions containing these polyelectrolytes. The fact that it is possible to obtain multilayers must be attributed to the overcharging of the surface every time when a new layer is adsorbed onto the substrate. Our calculations now provide the theoretical explanation for the possibility to form these multilayers. Earlier it was argued that there should exist a critical ionic strength above which the overcharging does not take place. Therefore, our theory predicts that only stable multilayers can form when the ionic strength is sufficiently low. Inspection of the available literature confirms this prediction.[19] Stable multilayers can only form when the ionic strength is below a critical value.

The results presented are just the first results obtained by the two-gradient method and do not constitute a complete analysis. Nevertheless, the results clearly indicate that it is possible to construct the adsorption isotherms for branched polyelectrolytes, micelles, and other highly charged objects with the account of lateral correlations. The most important new ingredient in the present analysis is the treatment of the bulk chains. In the classical polyelectrolyte theory, the bulk chains are considered to be Gaussian chains ''living'' at homogeneous (zero) electrostatic potential. The equilibration of adsorbed polyelectrolyte chains with the ideal bulk chains resulted in the failure to retain sufficient chains on the surface to overcompensate the surface charge. In the present theory the intramolecular excluded volume as well as the electrostatics inside and around the bulk chains is (on a mean field level) accounted for. Bringing adsorbed chains in equilibrium with the more realistic bulk chains has the result that the chains remain on the surface even when the electrostatic potential is against it, e.g., when there is some overcompensation of the charge. Consequently, the success of the present theory to convincingly predict overcompensation of the surface charge by adsorbed polyelectrolyte must in part be attributed to the improved way in which the bulk chains are equilibrated with the adsorbed chains. The possibility to account for lateral inhomogeneities in the adsorbed layer

(which may be called lateral correlations) is a second aspect which contributes to the overcharging mechanism.

The equilibrium structure of such adsorbed layers is, as expected, rather complicated due to both the electrostatic and the steric interactions with the surface. It is significant to reiterate that it was shown here that the adsorbed layer is not, as predicted by the classical theory, very thin. Even when the surface is starved (undersaturated), the stars on the surface are only weakly deformed as compared to the stars in the bulk. The deformation can of course increase when the charge density on the surface exceeds the projected charge density of the star. Then the star collapses onto the surface and forms a thin layer. We believe that these observations are important new findings that can be tested experimentally.

Application of the present theory to the adsorption of linear polyelectrolytes is possible. However, it is expected that the two-gradient SCF model is less accurate for the linear case than for the star-like polyelectrolyte. The reason for this is clear. When the star has sufficient number of arms, it must remain roughly spherical. The linear chain can deviate significantly from the spherical shape, especially when the charge density along the chain is high. Nevertheless, we believe that the present approach may serve as a good starting point to revisit several regimes in polyelectrolytes at interface, where both electrostatic and nonelectrostatic interactions are present. Work along these lines is in progress.

V. CONCLUSIONS

We have shown that SCF theory can be used to find overcompensation of the surface charge by adsorbing polyelectrolyte stars. This overcompensation occurs at low ionic strength conditions and when the projected charge density of the star is higher than the charge density of the surface. The key ingredient in the theory responsible for the charge overcompensation is that intramolecular excluded-volume effects of both stars near the surface and stars in the bulk are accounted for (in an approximate way). This improved method may be used to construct the adsorption isotherms for branched polyelectrolytes, micelles, and other highly charged objects with the account of lateral correlations between them. The equilibrium structure of such adsorbed layers turns out to be rather complicated due to both the electrostatic and steric interactions with the surface. It has been shown that the outer part of the adsorbed layer has much in common with outer edges of stars in solution. For example the charge is locally compensated by the counterions of the star. We aim to perform a more detailed analysis of such systems in our future publications.

ACKNOWLEDGMENTS

The authors would like to thank Oleg Borisov for many stimulating discussions. This work was partially supported by the NWO Dutch-Russian Project No. 500012 ''Self-organization and Structure of Bio-nanocomposites.'' E.B.S. acknowledges financial support from the National Science Foundation (Grant No. DMR-9973300).

[1] J. Papenhuijzen, H. A. van der Schee, and G. J. Fleer, J. Colloid Interface Sci. **104**, 540 (1985).
[2] O. A. Evers, G. J. Fleer, J. M. H. M. Scheutjens, and J. Lyklema, J. Colloid Interface Sci. **111**, 446 (1986).
[3] M. R. Böhmer, O. A. Evers, and J. M. H. M. Scheutjens, Macromolecules **23**, 2288 (1990).
[4] V. Shubin and P. Linse, Macromolecules **30**, 5944 (1997).
[5] H. G. M. van de Steeg, M. A. Cohen Stuart, A. de Keizer, B. H. Bijsterbosch, Langmuir **8**, 2538 (1992).
[6] I. Borukhov, D. Andelman, and H. Orland, Macromolecules **31**, 1665 (1998).
[7] A. Yu. Grosberg, T. T. Nguyen, and B. I. Shklovskii (unpublished).
[8] M. Jonsson and P. Linse, J. Chem. Phys. **115**, 3406 (2001).
[9] T. T. Nguyen, A. Yu. Grosberg, and B. I. Shklovskii, J. Chem. Phys. **113**, 1110 (2000).
[10] R. M. Talingting, Y. Ma, C. Simmons, and S. E. Webber, Langmuir **16**, 862 (2000).
[11] J. N. Israelachvili, *Intermolecular and Surface Forces* (Academic, London, 1985).
[12] O. V. Borisov, J. Phys. II **6**, 1 (1996); J. Klein Wolterink, F. A. M. Leermakers, G. J. Fleer, L. K. Koopal, E. B. Zhulina, and O. V. Borisov, Macromolecules **32**, 2365 (1999).
[13] O. V. Borisov, F. Hakem, T. A. Vilgis, J.-F. Joanny, and A. Johner, Eur. Phys. J. E (to be published).
[14] N. M. Maurits, J. G. E. M. Fraaije, P. Altevogt, and O. A. Evers, Comput. Theor. Polym. Sci. **6**, 1 (1996).
[15] G. Decher and J. D. Hong, Makromol. Chem., Macromol. Symp. **46**, 321 (1991).
[16] G. Decher and J. D. Hong, Ber. Bunsenges. Phys. Chem. **95**, 1430 (1991).
[17] G. Decher, J. D. Hong, and J. Schmitt, Thin Solid Films **201/211**, 831 (1992).
[18] N. G. Hoogeveen, M. A. Cohen Stuart, G. J. Fleer, and M. R. Böhmer, Langmuir **12**, 3675 (1996).
[19] D. Kovacevic, S. van der Burgh, A. de Keizer, and M. A. Cohen Stuart, Langmuir **18**, 5607 (2002).